Macromolecules

COMMUNICATION TO THE EDITOR

pubs.acs.org/Macromolecules

Semiconductor−Insulator−Semiconductor Sandwiched Lozenge Crystals of Poly(3-butylthiophene)-*block*-polyethylene Copolymer

Yuzhen Wang,[†,‡,§] Jiayue Chen,[†,‡,§] Sijun Li,[†,‡,§] Ligui Li,[†,‡,§] Qing Su,[†,‡] Jie Wang,[†,‡] and Xiaoniu Yang*[,†,‡]

[†]Polymer Composites Engineering Laboratory, Changchun Institute of Applied Chemistry, Chinese Academy of Sciences, Renmin Str. 5625, Changchun 130022, P. R. China

[‡]State Key Laboratory of Polymer Physics and Chemistry, Changchun Institute of Applied Chemistry, Chinese Academy of Sciences, Renmin Str. 5625, Changchun 130022, P. R. China

[§]Graduate University of the Chinese Academy of Sciences, Beijing 100049, P. R. China

Supporting Information

INTRODUCTION

Conjugated polymers, especially regioregular poly(3-alkylthiophenes) (P3ATs), have demonstrated intriguing electrical and optical properties for broad applications in high performance organic thin film transistors, polymer solar cells, and chemical sensors.[1−3] In attempt to improve both the mechanical and processing properties, a group of regioregular P3AT-based rod−coil diblock copolymers have been developed, and its functionality in electronic devices has also been examinied.[4,5] These materials not only show better mechanical property and reduced cost as their inherent advantage corresponding to their molecular design but also are able to preserve the excellent electric and optoelectric properties of P3ATs despite the presence of the nonconjugated segments.[4] By utilizing self-assembling capability of morphology formation associated with rod−coil block copolymers,[6] the molecular packing and microscopic morphology of polythiophene in the solid films or solutions, which play an important role in determining their properties in the devices, can be well controlled. However, the previous study mainly focused on P3AT−amorphous diblock copolymers. Microphase separation with crystalline whiskers and amorphous domains are frequently observed in these block copolymers, e.g., P3HT-*b*-PMA,[4] P3HT-*b*-PS,[5] and P3HT-*b*-PI.[5] Compared with the self-assembled P3AT copolymers having an amorphous block, it is highly expected to obtain novel morphology from the copolymers with crystallizable block, such as polyethylene (PE), by using the competition between the crystallization and phase separation processes of the blocks, to achieve novel properties and applications.[7−9] The crystallization or melting of diblock copolymers with one or both crystallizable segments, e.g., PEO-*b*-PS,[10−12] PCL-*b*-PB,[13] and PEG-*b*-PCL,[14] has been extensively studied so far. It is well-known that polyethylene is one of the insulating polymers with strong crystallizability. Muller et al. have reported that semiconducting diblock copolymer consisting of polyethylene and regioregular poly(3-hexylthiophene) (P3HT) segments P3HT-*b*-PE demonstrated a rich phase behavior, high charge carrier mobility, and on−off ratios as well as outstanding mechanical properties even at 90 wt % insulating polyethylene moiety.[8] The crystallization behavior and solid-state morphology of P3HT-*b*-PE copolymer from the melt have also been reported.[9] However, the crystallization of these polyethylene-based block copolymers from dilute solution has seldom been studied yet. One might naturally flash in this mind whether the typical morphology of solution crystallized polyethylene, lozenge or truncated lozenge crystals could also be achieved from these block copolymers, and how will P3AT block organize with those polyethylene lamellae? To disclose these questions, a poly(3-butylthiophene) (P3BT)-based polyethylene diblock copolymer P3BT-*b*-PE is synthesized in this work. The reason to choose P3BT instead of much more studied P3HT is due mainly to the higher crystallinity of P3BT segment, which entitles this diblock copolymer with both crystalline−crystalline and insulating−semiconducting[15] characteristics.

EXPERIMENTAL PART

The synthesis of P3BT-*b*-PE diblock copolymer was carried out according to a similar method previously reported by Radano et al.[7] The detailed synthetic procedures and molecular structure characterization are presented in the Supporting Information. Homopolyethylene as a reference was prepared by using a Cp_2ZrCl_2/MAO catalytic system.[16] Molecular weights, polydispersities, and their thermal data of all the samples are listed in Table 1. $BT_{25}bE_{75}$ represents the P3BT-*b*-PE diblock copolymer with a P3BT block weight fraction of 25%. A nonisothermal solution crystallization technique was utilized to prepare crystals of P3BT-*b*-PE diblock polymer. $BT_{25}bE_{75}$ was dissolved in hot *o*-dichlorobenzene (ODCB) at 120 °C for 20 min to give a solution with a concentration of 10 mg/mL. Thus, the obtained solution was subsequently cooled to room temperature within 5 min. For comparison, single crystals of polyethylene have also been prepared by using the self-seeding method.[19] Thus, obtained single crystals were deposited on TEM copper grids coated with a thin amorphous carbon layer or on precleaned silicon wafers (1 cm × 1 cm) for further observation without filtration. The surface decoration method by using a low molecular weight polyethylene (M_n = 15 kg/mol, M_w/M_n = 1.12)[20] was utilized to reveal the surface topography of lamellar crystals. The morphology characterization was carried out on an Olympus BX-51 optical system microscope (Tokyo, Japan) and transmission

Received: January 21, 2011
Revised: February 20, 2011
Published: March 15, 2011

Table 1. Molecular Structure Characterization and Thermal Properties of P3BT-*b*-PE, Homo-P3BT, and Homo-PE

				PE[d]			P3BT[d]		
sample	M_n (kg/mol)	M_w/M_n	W_{P3BT} (%)	T_m (°C)	T_c (°C)	X_c[e]	T_m (°C)	T_c (°C)	X_c[e]
PE	9.7[a]	2.58[a]		133	118.4	0.594			
$BT_{25}bE_{75}$	29.2[b]	1.32[c]	25[b]	123.8	104.4	0.349	244.4	202.3	0.148
P3BT	7.3[c]	1.13[c]	100				252.3	217.8	0.20

[a] As determined by GPC with 1,2,4-trichlorobenzene as the eluent at 130 °C. [b] As determined by ^{1}H NMR spectroscopy using the molecular weight of the P3BT precursor (M_n = 7.3 kg/mol) obtained by GPC in THF. [c] Number-average molecular weight (M_n) and polydispersity index (M_w/M_n) determined by GPC with THF as the eluent and polystyrene as standard. [d] Phase transition temperature of PE block and P3BT block was measured by DSC thermogram at heating and cooling rate of 10 °C/min. [e] Crystallinity determined from X_c (%) = ($\Delta H_m/\Delta H_m^*$) × 100, ΔH_m^*(PE) = 290 J/g,[17] ΔH_m^*(P3BT) = 112 J/g from the linear extrapolation of the P3AT data.[18]

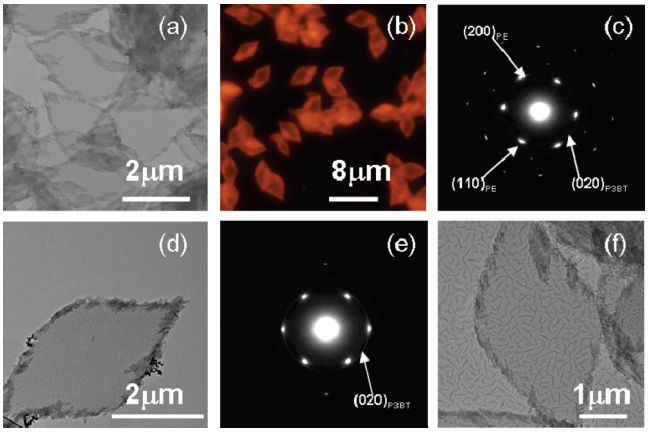

Figure 1. Morphology of $BT_{25}bE_{75}$ diblock copolymer lozenge crystals prepared via cooling 10 mg/mL *o*-dichlorobenzene solution from 120 °C to room temperature: (a) bright-field (BF) TEM image; (b) representative fluorescence microscopy image; (c) selected-area electron diffraction (SAED); (d) BF-TEM image upon annealing at 102 °C and (e) corresponding SAED; (f) BF-TEM image of the single crystal decorated with low molecular weight polyethylene rods.

electron microscope (JEOL JEM-1011) equipped with a CCD camera at an accelerating voltage of 100 kV. The evolution process of $BT_{25}bE_{75}$ and homo-polyethylene single crystals was carried out on Agilent 5500 scanning probe microscope equipped with a high-temperature heating module under a N_2 atmosphere.

RESULTS AND DISCUSSION

Typical morphology of $BT_{25}bE_{75}$ crystals formed by cooling 10 mg/mL *o*-dichlorobenzene solution from 120 °C to room temperature is shown in Figure 1. Lozenge crystal, which is the typical morphology of polyethylene single crystals as grown from dilute solution,[21] is also obtained from this $BT_{25}bE_{75}$ diblock copolymer. This morphology is obviously different from those cases observed in the other diblock copolymers containing a P3AT segment and another amorphous block.[4,5] The sizes of these $BT_{25}bE_{75}$ lozenge crystals are about 4 μm in length and 2.5 μm in width. The rounded edges of the growth fronts, which frequently appeared in both melt- and solution-grown polyethylene single crystals at high crystallization temperatures,[22−24] are also observed. The central pleats or corrugation lines, which are characteristic morphology of the polyethylene lozenge,[25] however, are not observed in these crystals. As illustrated in the fluorescence image (Figure 1b), it is found that every $BT_{25}bE_{75}$ lozenge crystal is highly fluorescent, implying that conjugated P3BT is chemically linked to PE. In order to determine the structure of $BT_{25}bE_{75}$ single crystals and the composition distribution, we resorted to selected-area electron diffraction measurements (SAED). As shown in Figure 1c, there are distinct (110) and (200) diffraction spots from polyethylene crystal,[25] indicating PE chains adopt normal orientation to the lamella. A weak diffraction ring originated from the reflection of crystallographic (020) plane of poly(3-butylthiophene) crystals can be distinguished, which implies that $\pi-\pi$ stacking direction is random in $BT_{25}bE_{75}$ single crystals.[1] After annealing at 102 °C (Figure 1d,e), $BT_{25}bE_{75}$ crystals maintain lozenge morphology, and the typical electron diffraction spots of polyethylene single crystal, i.e., (110) and (200), can also be observed with comparable intensity to those shown in Figure 1c. However, the (020) reflection intensity of P3BT is substantially increased, suggesting that higher crystallinity is obtained and the linkage to polyethylene block is still preserved. Therefore, no epitaxial relationship exists between polyethylene and P3BT crystals.[26] To further ascertain the distribution of P3BT within this lozenge crystal, low molecular weight polyethylene was thermally evaporated onto these $BT_{25}bE_{75}$ crystals. After the deposition of low molecular weight polyethylene, a lot of rodlike polyethylene crystals are found randomly distributing on the top surface of these lozenge crystals, which is in contrast to that perfect sector-specific alignment observed in conventional polyethylene lozenge crystals,[20] as shown in Figure 1f. Moreover, after careful comparison by using high-magnification TEM and AFM, we can observe that the surfaces of $BT_{25}bE_{75}$ lozenge crystals are covered with many short P3BT whiskers (Figure S5a−d). Obviously, $BT_{25}bE_{75}$ lozenge crystals have rougher surface than those of homopolyethylene crystals (Figure S5e). Therefore, we speculate that there is no apparent alignment of the P3BT lamellae on the surface of these lozenge crystals. On the basis of the above observations, we can conclude that PE blocks will first fold to form lozenge mats. As a result, P3BT blocks are excluded from polyethylene mats to both the top and bottom surfaces of the polyethylene crystals to form a semiconducting−insulating−semiconducting triple-layer structure. It should be pointed out that polyethylene lozenge crystals are usually obtained in dilute solution via isothermal crystallization. However, in the present study, these lozenge crystals composed of $BT_{25}bE_{75}$ diblock copolymer are grown from relatively concentrated solution. It is speculated that the well-dissolved P3BT segments on polyethylene blocks nuclei may create a region with relatively low concentration of crystallizable polyethylene chains, which is beneficial to the formation of perfect single crystals. The study of detailed thermodynamic and kinetic process of crystallization is ongoing.

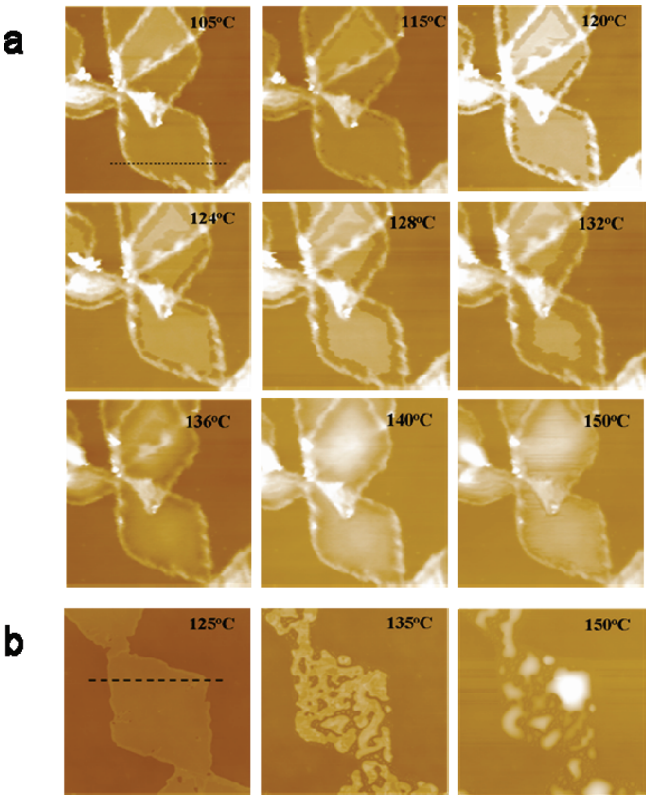

Figure 2. A series of AFM height images taken in situ at various temperatures showing the annealing and melting process of $BT_{25}bE_{75}$ (panel A) and homopolyethylene (panel B) lozenge crystals on a silicon substrate (insets are the annealing and melting temperatures). The images were taken at 30 min after the specimen was heated to corresponding temperature. Cross-sectional profile data were obtained by scanning along the lines in the AFM images and will be shown in Figure 3. Scan sizes are 5 μm × 5 μm for panel A and 6 μm × 6 μm for panel B.

The thermal behaviors of $BT_{25}bE_{75}$ lozenge crystals were investigated by in-situ atomic force microscopy (AFM). A sequence of AFM height images of $BT_{25}bE_{75}$ and homopolyethylene lozenge crystals at elevated temperatures are presented in Figure 2. No morphological change could be observed before the $BT_{25}bE_{75}$ crystals have been heated to 105 °C (Figure 2a). Scattered holes start to develop on the edge of the crystals at 115 °C. With further heating to 128 °C, these holes become larger and merge each other, leading to the formation of a ring gap which separates the lozenge into inner and outer parts. It should be noted here that surface texture at the four sectors of these lozenge crystals are totally the same, with a comparable disintegration speed perpendicular to the {110} growth front associated with four sectors. Therefore, the melting process does not change the morphology, at least the shape of the lozenge crystals, except the increased height of the central area, as proven by the topography obtained from 124 to 132 °C. Further increasing the temperature will eventually cause the crystals to melt at 136 °C, and only a liquid massif is observed at 150 °C, which is still enveloped by unmelted P3BT. Upon cooling from the molten state, fibrillar lamellae with identical thickness are observed in the whole area (Figure S6a). As a reference, the thermal behaviors of polyethylene lozenge crystals prepared via the self-seeding method were also investigated by using in-situ AFM measurement. Three typical morphological evolution stages, which are consistent with previous results in TEM and AFM studies, are presented in Figure 2b.[27−30] Sawtooth edge can only be observed as the homopolyethylene crystals have been heated up to 125 °C. After heating up to 135 °C for several minutes, lots of large holes randomly distribute all over the lozenge, and the thickened lamellae do not move out across the lozenge rim of the original lamella. At 150 °C, they melt into several droplets with different sizes. When the specimen was cooled from the molten state, lamellae grew within the droplets, and small globules became more notable on the thin layer (Figure S6b), whereas the holes are found on the $BT_{25}bE_{75}$

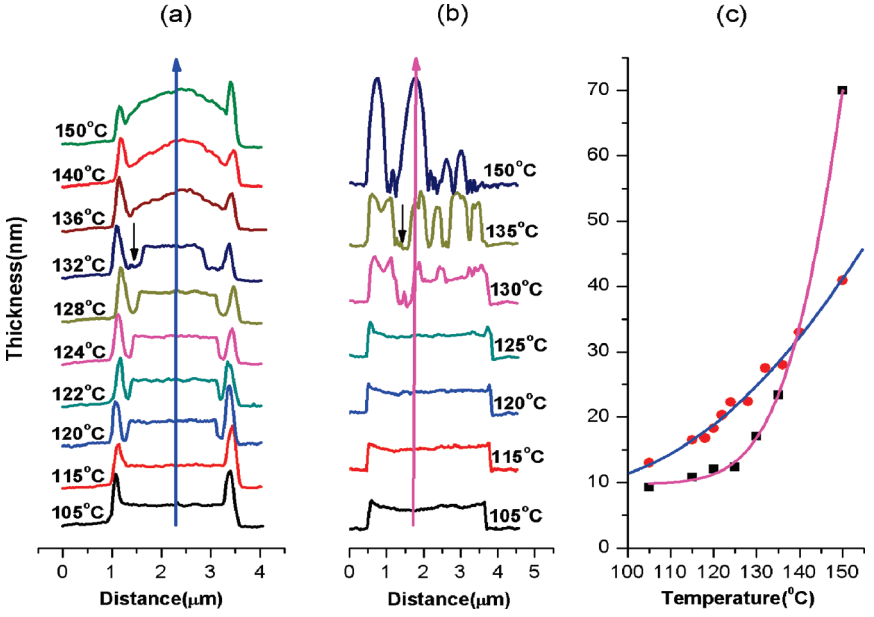

Figure 3. Cross-section profile data of (a) $BT_{25}bE_{75}$ and (b) homopolyethylene lozenge crystals at different annealing temperatures corresponding to the dotted lines marked in Figure 2. (c) Dependence of thickness on annealing temperature. ● and ■ denote $BT_{25}bE_{75}$ and homopolyethylene, respectively. Thickness is measured at corresponding marked arrow lines (blue for (a) and pink for (b)).

dx.doi.org/10.1021/ma200153b |*Macromolecules* 2011, 44, 1737–1741

crystals at a relatively low temperature of 115 °C. Therefore, this observation is consistent with previously demonstrated DSC scans that melting temperature of polyethylene blocks decreases upon blocking with P3BT.

In addition to the distinct morphological differences between $BT_{25}bE_{75}$ and homopolyethylene lozenge crystals during thermal annealing, we also note that the thickening process in both crystals is rather different. From the series of height histograms of $BT_{25}bE_{75}$ crystals taken from the same position marked by the dotted line in Figure 2a (Figure 3a), it is observed that the surface of the inner part of lozenge crystals is quite smooth and with a height of ca. 13 nm at 105 °C. When the temperature is increased to 115 °C, the thickness of this area is increased to 16.5 nm, accompanying by the emergence of some holes at the boundary. These holes gradually develop toward the center of crystals upon further heating, leaving behind about 10 nm viscous fluid layer (black arrow in Figure 3a). Interestingly, in contrast to the melting process occurring on the crystal edges, the rest central part not only preserves its solid state with smooth surface but also becomes thicker simultaneously. Whereas for the homopolyethylene lozenge crystals, as indicated by the cross-section profile in Figure 3b, the holes which reach the substrate surface (black arrow in Figure 3b) will appear when temperature is gradually increased, resulting in a holey film with increased thickness around the holes. To give a vivid comparison for these two samples, the thickness dependence of certain sites on temperature is given in Figure 3c. In both cases, the lozenge crystals become thicker upon heating. However, the thickness of the lamellae of homopolyethylene lozenge crystals suddenly increases when the annealing temperature is increased to ca. 130 °C, while the thickening speed of $BT_{25}bE_{75}$ crystals is relatively slow in the whole heating process. We ascribe this characteristic thickening process of $BT_{25}bE_{75}$ crystals to the existence of P3BT whiskers on the lamellar surface, which has a tendency to maintain polyethylene block to its lattice positions since the melting temperature of P3BT segment is far higher than that of polyethylene block. Interestingly, for the crystalline−amorphous (coil) diblock copolymers, such as PCL-*b*-PB, the competition between the lamellar thickening and the contraction of the coil block on heating leads to a constant long spacing.[13] This is totally different from the situation in $BT_{25}bE_{75}$ lozenge crystals, probably due to the P3BT block is crystalline and the melting temperature is very high.

To have a better understanding on the morphological transformations resulted from the chain unfolding during thermal annealing, ex-situ annealing of $BT_{25}bE_{75}$ and homopolyethylene lozenge crystals was carried out at different temperatures. TEM images (Figure S8) were recorded as the samples have been cooled to room temperature. Morphological evolution of both crystals is in good agreement with AFM data. However, $BT_{25}bE_{75}$ crystals are still able to preserve their integrity even at 250 °C, in contrast to that of homopolyethylene crystals. On the basis of the above observations, the following mechanism is proposed to account for the characteristic thickening of $BT_{25}bE_{75}$ lozenge crystals. Annealing at low temperatures makes polyethylene block at the edge melt first because of relative less confinement and thus higher segment mobility.[31] Compared with homopolyethylene, it is impossible for polyethylene blocks with a linkage to the rigid rod to transport over appreciable distances to recrystallize into a thickened rim on the edge of the unmelted region. With further increased temperature, polyethylene blocks keep on melting stage and are likely covered by a layer of rigid P3BT. The slower thickening of unmelted part might be attributed to the poorer chain mobility of polyethylene blocks under vertical confinement, leaving those segments are only able to reorganize locally within a relatively tiny region.

In conclusion, the uniform solution-grown lozenge crystals of $BT_{25}bE_{75}$ block copolymers have been prepared via the non-isothermal solution crystallization method. These lozenge crystals are covered with semiconductive P3BT layers at both sides, forming semiconductor−insulator−semiconductor sandwiched morphology. Thus, these crystals are much more stable upon thermal annealing in comparison with those lozenges of homopolyethylene due to the confinement of P3BT layers. This electrically sandwiched morphology shows potential applications in microscale capacitors and other organic optoelectronic devices.

■ ASSOCIATED CONTENT

Supporting Information. Details of synthesis and characterization of P3BT-*b*-PE and AFM data. This material is available free of charge via the Internet at http://pubs.acs.org.

■ AUTHOR INFORMATION

Corresponding Author
*E-mail: xnyang@ciac.jl.cn.

■ ACKNOWLEDGMENT

This work was financially supported by National Natural Science Foundation of China (Grants 20874100, 20925415, and 20990233). We thank the Fund for Creative Research Groups (Grant 50921062) and Solar Energy Initiative (Grant KGCX2-YW-399+9) of the Chinese Academy of Sciences for financial support.

■ REFERENCES

(1) McQuade, D. T.; Pullen, A. E.; Swager, T. M. *Chem. Rev.* **2000**, *100*, 2537–2574.
(2) Murphy, A. R.; Frechet, J. M. J. *Chem. Rev.* **2007**, *107*, 1066–1096.
(3) Gunes, S.; Neugebauer, H.; Sariciftci, N. S. *Chem. Rev.* **2007**, *107*, 1324–1338.
(4) Sauve, G.; McCullough, R. D. *Adv. Mater.* **2007**, *19*, 1822–1825.
(5) Iovu, M. C.; Craley, C. R.; Jeffries-EL, M.; Krankowski, A. B.; Zhang, R.; Kowalewski, T.; McCullough, R. D. *Macromolecules* **2007**, *40*, 4733–4735.
(6) Lee, M.; Cho, B. K.; Zin, W. C. *Chem. Rev.* **2001**, *101*, 3869–3892.
(7) Radano, C. P.; Scherman, O. A.; Stingelin-Stutzmann, N.; Muller, C.; Breiby, D. W.; Smith, P.; Janssen, R. A. J.; Meijer, E. W. *J. Am. Chem. Soc.* **2005**, *127*, 12502–12503.
(8) Muller, C.; Goffri, S.; Breiby, D. W.; Andreasen, J. W.; Chanzy, H. D.; Janssen, R. A. J.; Nielsen, M. M.; Radano, C. P.; Sirringhaus, H.; Smith, P.; Stingelin-Stutzmann, N. *Adv. Funct. Mater.* **2007**, *17*, 2674–2679.
(9) Muller, C.; Radano, C. P.; Smith, P.; Stingelin-Stutzmann, N. *Polymer* **2008**, *49*, 3973–3978.
(10) Zhu, L.; Cheng, S. Z. D.; Calhoun, B. H.; Ge, Q.; Quirk, R. P.; Thomas, E. L.; Hsiao, B. S.; Yeh, F. J.; Lotz, B. *J. Am. Chem. Soc.* **2000**, *122*, 5957–5967.
(11) Chen, W. Y.; Li, C. Y.; Zheng, J. X.; Huang, P.; Zhu, L.; Ge, Q.; Quirk, R. P.; Lotz, B.; Deng, L. F.; Wu, C.; Thomas, E. L.; Cheng, S. Z. D. *Macromolecules* **2004**, *37*, 5292–5299.

(12) Hsiao, M. S.; Chen, W. Y.; Zheng, J. X.; Van Horn, R. M.; Quirk, R. P.; Ivanov, D. A.; Thomas, E. L.; Lotz, B.; Cheng, S. Z. D. *Macromolecules* **2008**, *41*, 4794–4801.
(13) Nojima, S.; Kato, K.; Yamamoto, S.; Ashida, T. *Macromolecules* **1992**, *25*, 2237–2242.
(14) Sun, J. R.; Chen, X. S.; He, C. L.; Jing, X. B. *Macromolecules* **2006**, *39*, 3717–3719.
(15) Budianto, Y.; Aoki, A.; Miyashita, T. *Macromolecules* **2003**, *36*, 8761–8765.
(16) Kaminsky, W.; Steiger, R. *Polyhedron* **1988**, *7*, 2375–2381.
(17) Darras, O.; Seguela, R. *Polymer* **1993**, *34*, 2946–2950.
(18) Malik, S.; Nandi, A. K. *J. Polym. Sci., Part B: Polym. Phys.* **2002**, *40*, 2073–2085.
(19) Blundell, D. J.; Keller, A.; Kovacs, A. J. *J. Polym. Sci., Part B: Polym. Lett.* **1966**, *4*, 481–486.
(20) Wittmann, J. C.; Lotz, B. *J. Polym. Sci., Part B: Polym. Phys.* **1985**, *23*, 205–226.
(21) Bassett, D. C. *Principles of Polymer Morphology*; Cambridge University Press: New York, 1981.
(22) Toda, A. *Faraday Discuss.* **1993**, 129–143.
(23) Ungar, G.; Putra, E. G. R. *Macromolecules* **2001**, *34*, 5180–5185.
(24) Organ, S. J.; Keller, A. *J. Mater. Sci.* **1985**, *20*, 1571–1585.
(25) Geil, P. H. *Polymer Single Crystals*; John Wiley & Sons: New York, 1963.
(26) Kyo, J. I.; Paul, S. *Bull. Inst. Chem. Res., Kyoto Univ.* **1991**, *69*, 111–116.
(27) Organ, S. J.; Hobbs, J. K.; Miles, M. J. *Macromolecules* **2004**, *37*, 4562–4572.
(28) Magonov, S. N.; Yerina, N. A.; Ungar, G.; Reneker, D. H.; Ivanov, D. A. *Macromolecules* **2003**, *36*, 5637–5649.
(29) Nakamura, J.; Kawaguchi, A. *Macromolecules* **2004**, *37*, 3725–3734.
(30) Loos, J.; Tian, M. W. *Polymer* **2006**, *47*, 5574–5581.
(31) Winkel, A. K.; Hobbs, J. K.; Miles, M. J. *Polymer* **2000**, *41*, 8791–8800.